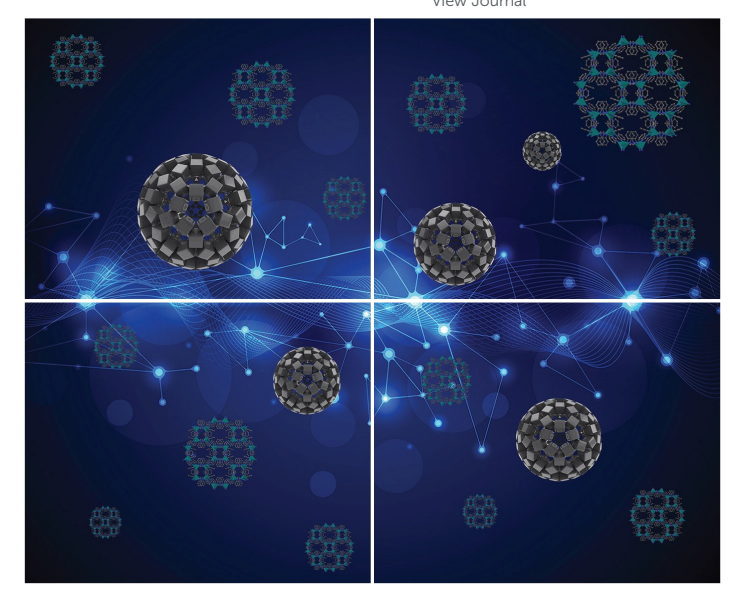
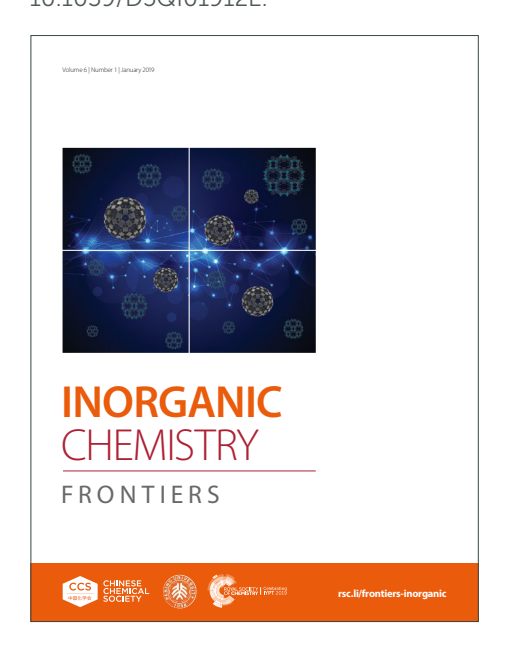
INORGANIC CHEMISTRY

FRONTIERS

Accepted Manuscript



This article can be cited before page numbers have been issued, to do this please use: H. Wen, M. Wang, X. Dong, Z. Xu, Y. Geng, J. Qin, J. Luo, M. Zhang and L. Li, *Inorg. Chem. Front.*, 2026, DOI: 10.1039/D5QI01912E.



This is an Accepted Manuscript, which has been through the Royal Society of Chemistry peer review process and has been accepted for publication.

Accepted Manuscripts are published online shortly after acceptance, before technical editing, formatting and proof reading. Using this free service, authors can make their results available to the community, in citable form, before we publish the edited article. We will replace this Accepted Manuscript with the edited and formatted Advance Article as soon as it is available.

You can find more information about Accepted Manuscripts in the <u>Information for Authors</u>.

Please note that technical editing may introduce minor changes to the text and/or graphics, which may alter content. The journal's standard <u>Terms & Conditions</u> and the <u>Ethical guidelines</u> still apply. In no event shall the Royal Society of Chemistry be held responsible for any errors or omissions in this Accepted Manuscript or any consequences arising from the use of any information it contains.







View Article Online DOI: 10.1039/D5QI01912E

Inorganic Chemistry Frontiers Accepted Manuscript

SCHOLARONE™ Manuscripts

View Article Online DOI: 10.1039/D5QI01912E

ARTICLE

Halogen-bond induced polar multilayer hybrid perovskites for efficient self-driven X-ray detection

Received 00th January 20xx. Accepted 00th January 20xx

DOI: 10.1039/x0xx000000x

Haotian Wen, a,b Minmin Wang, a,b Xin Dong,b Zhijin Xu,b Yaru Geng,b Jie Qin, a,b Junhua Luo, b,d Min Zhang, *a,c,d and Lina Li *a,b,d

Two-dimensional (2D) hybrid perovskites possess remarkable X-ray absorption and outstanding carrier transport properties, show-ing great application prospects in efficient X-ray detection. However, most 2D hybrid perovskites require an external voltage to achieve X-ray detection, resulting excessive device power dissipation and pronounced ion migration effects. Thus, it is necessary to develop novel self-driven X-ray detection materials. Here, by alloying iodine-substituted cations I-BA, (I-BA = 4-iodobutylammonium) instead of n-butylamine cations into MAPbl₃ (MA = methylammonium), a 2D triple-layer polar hybrid per-ovskite (I-BA)₂(MA)₂Pb₃I₁₀ (1) is acquired. Due to the introduction of iodine-substituted amines, additional noncovalent I···H hydrogen bonds between organic cations and I···I halogen bonds between cations and inorganic halides are formed, endowing 1 with a polar structure. Notably, 1 delivers a 0.15 V open-circuit photovoltage under X-ray irradiation and features self-driven X-ray detection behavior. Furthermore, 1 demonstrates a high sensitivity of 221.7 μC Gy¹ cm⁻² with a low limit of detection of 16.3 nGy s⁻¹. The distinctive characteristics of 1 render it an excellent candidate for self-driven Xray detection, simultaneously offering valuable guidance for the precise design of advanced X-ray detection materials.

Introduction

X-ray detectors serve critical functions across multiple essential domains, particularly in medical diagnostics, non-destructive product evaluation, security inspections, and scientific investigations. 1-6 Consequently, developing novel materials for improved X-ray detection continues to be a major focus of global research efforts.7 Lead halide perovskites have recently gained prominence in direct X-ray detection applications owing to their facile synthesis,8 strong X-ray attenuation capabilities,9-¹¹ and superior optoelectronic performance. ¹²⁻¹⁶ However, the reliance of most detectors on strong electric fields often causes severe ion migration, resulting in unstable performance, increased energy consumption, and bulkv circuit configurations. 15, 17, 18 Therefore, the development of selfdriven devices capable of operating without an external bias voltage has attracted growing attention in X-ray detection. 19

Traditionally, constructing a p-n heterojunction can generate a spontaneous potential gradient, which leads to photo-induced charge separation and drift for self-driven supply.²⁰⁻²³ However, the complexity of the manufacturing process and interface engineering hinders the large-scale application of this

perovskites through non-covalent interactions is promising.

method.²⁴ Alternatively, introducing chiral organic cations induces the crystallization of the resulting perovskite into a chiral-polar point group, thus naturally endowing the compound with polar characteristics to generate self-driven photodetection. For in-stance, self-driven circular polarization photodetection with high sensitivity was achieved in (R-PPA)EAPbBr₄.²⁵ Then, Wu et al. successfully achieved self-driven X-ray detection in chiral-polar (R-MPA)₄AgBil₈,²⁶ which holds great promise for self-driven X-ray detector. Nevertheless, enantiopure chiral organic ammonium cations obtained through asymmetric synthesis and chiral separation are often scarce and expensive. Therefore, self-driven detection materials constructed based on achiral cations are still highly desired. In lead halide perovskites, non-covalent interactions (steric hindrance, π - π interaction, hydro-gen bond, van der Waals force)^{27, 28} among organic cations and those (electrostatic interaction, hydrogen bond, halogen bond)^{29, 30} between cations and inorganic halides influence the physical properties of the crystal. For instance, Liu et al. introduced carboxylic acid group to construct quasi-Ruddlesden-Popper motifs with reduced energy gaps via strong O-H···O hydrogen bonds between adjacent spacer cations.31 In addition, carboxylic acid dimers significantly enhanced structural rigidity, thereby mitigating non-radiative recombination induced by tensile vibrations.³² The bromine-substituted organic cations were employed to enhance the molecular dipole moment, hindering oxygen atom diffusion and charged ion migration, leading to improved both chemical and operational stability.³³ Given that directional non-covalent interactions play a crucial role in guiding the crystal structure,34 inducing polarity in hybrid

^{a.} College of Chemistry, Fujian University, Fuzhou 350116, China.

b. State Key Laboratory of Functional Crystals and Devices, Fujian Institute of Research on the Structure of Matter, Chinese Academy of Sciences Fuzhou, Fujian,

^c State Key Laboratory of Structural Chemistry, Fujian Institute of Research on the Structure of Matter, Chinese Academy of Sciences, Fuzhou 350002, China.

d. Fujian Science & Technology Innovation Laboratory for Optoelectronic Information of China Fuzhou, Fujian, 350108, China.

ARTICLE Journal Name

Inspired by this, we present a polar trilayered perovskite $(I-BA)_2(MA)_2Pb_3I_{10}$ (1, where I-BA iodobutylammonium and MA = methylammonium), via incorporating iodine-replaced organic spacers. The noncovalent I···H hydrogen bonds between organic cations and I···I halogen bonds between cations and inorganic halides lead to 1 crystallization in a polar space group, thus enabling it to present self-driven photodetection. Moreover, the charge transport is enhanced through increasing the layers of the inorganic framework, thereby improving the self-driven photodetection performance. The high-quality single-crystal (SC) device exhibits a large photocurrent on-off ratio (5.74 \times 10³), a high responsivity (35.3 mA W⁻¹), and an outstanding detectivity (> 10¹² Jones) at 520 nm without an external bias voltage. Moreover, due to the excellent photo-response and the inorganic framework composed of heavy elements Pb and I, 1 demonstrates excellent self-driven X-ray detection capability, featuring a sensitivity of 221.7 μC Gy⁻¹ cm⁻², and an impressively low limit of detection (LoD) of 16.3 nGy s⁻¹. This work develops a strategy of inducing material polarity through haloamineincorporated enhancement of non-covalent interactions, paving the way for the design of exceptional self-driven X-ray detection materials.

Experimental

This article is licensed under a Creative Commons Attribution-NonCommercial 3.0 Unported Licence

Open Access Article. Published on 12 November 2025. Downloaded on 11/23/2025 5:16:22 PM

Pb(Ac)₂ (2.27 g, 6 mmol) was dissolved in 48% aqueous HI solution (10 mL) by heating to boiling under constant magnetic

stirring to give a yellowish solution. Subsequent addition of Aminobutanol (0.36 g, 4 mmol) and MA (0.45 g), 40 নি পার্নিত মি ভি থানি হ hot solution formed yellowish precipitation, which dissolved under stirring to afford a dark yellow solution. Moreover, which was subsequently dissolved by heating the solution to boiling. Finally, black-red crystals were obtained after the solution cooling to room temperature. For further details regarding the experimental and computational data, please consult the Supporting Information section.

Results and discussion

In HI solution, Pb(OAc)₂ was mixed with 4-aminobutanol and methylamine in stoichiometric ratios.³⁵ Through a gradual temperature reduction process, SCs of 1 were successfully grown, and the phase purity was confirmed by comparing the experimental PXRD pattern with the simulated pattern generated from the CIF (Figure S1, Supporting Information). Figure 1a illustrates the synthesis of 1 through iodine-mediated substitution of BA cations by I-BA cations. The introduction of heavy elements with a large atomic number (Z) increases the density to 3.62 g cm⁻³, which is higher than that of two-dimensional hybrid perovskites without halogensubstituted spacers, such as (BA)₂(MA)₂Pb₃I₁₀ (3.39 g cm⁻³),³⁶ (iBA)₂(MA)₂Pb₃I₁₀ (3.44 g cm⁻³, where iBA is isobutylamine),³⁷ and (PA)₂(MA)₂Pb₃I₁₀ (3.50 g cm⁻³, where PA is n-pentylamine).³⁸ Such high density is conducive to more efficient absorption of high-energy X-rays.

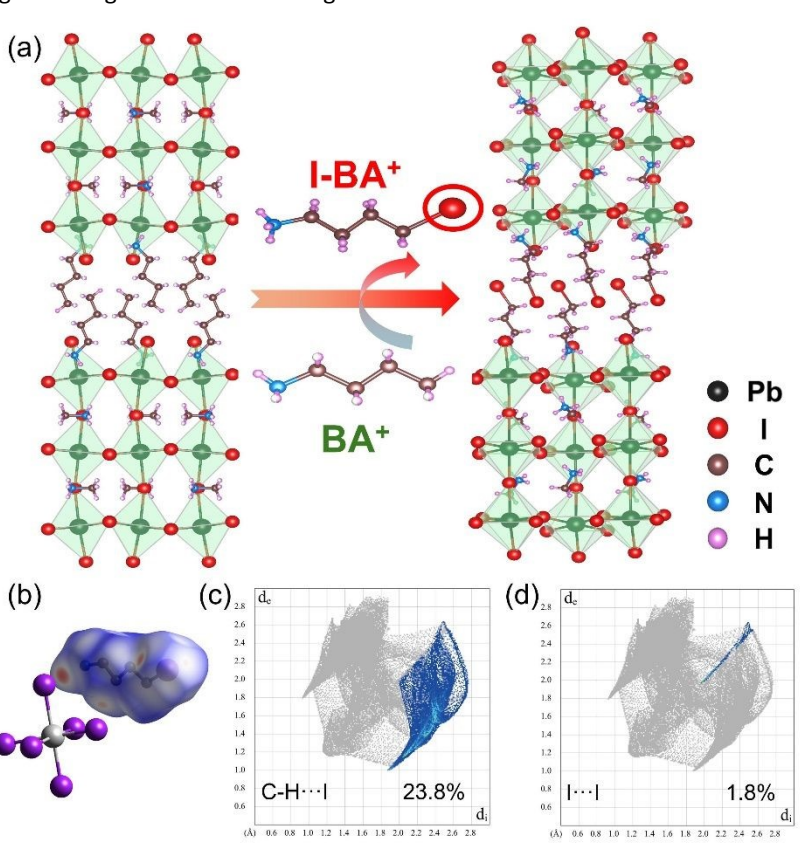


Fig. 1 (a) The iodine substitution strategy replaces BA cations with I-BA cations. (b) The Hirshfeld surface of I-BA cations in 1. (c) I····H, (d) I···I interactions.

norganic Chemistry Frontiers Accepted Manusc

Journal Name

ARTICLE

To further gain in-depth insights into the non-covalent interactions of I-BA cations in perovskites, we analyzed the Hirshfeld dnorm surface plot, 2D fingerprint plot (Figure 1b-d), and the interactions in 1 using Crystal Explorer software derived from the CIF file. Under the effect of iodine-substituted cations, additional interactions between layers were formed in 1 (Figure S2 and Figure S3, Supporting Information). As a result, the rotational freedom of the bulky cations was reduced to make them orient in an ordered manner, stabilizing 1 in a polar space group Pc. Meanwhile, through the point charge model calculation, the value of the electric polarization (P_s) along the c-axis of **1** was 3.62 μ C cm⁻² (Figure S4 and Table S1, Supporting Information), providing additional verification for its non-centrosymmetric structure (Figure S5, Supporting Information). Considering the polar structure of 1, it has great potential in self-driven photodetection.

To evaluate the potential of 1 in optoelectronic applications, absorption data for 1 were collected using UV-Vis spectroscopy (Figure S6, Supporting Information). 1 exhibited an absorption edge at approximately 720 nm. By fitting the Tauc's formula, we determined the optical bandgap of 1 to be 1.72 eV. Also, enabled by exceptionally well-formed SCs of 1, we constructed two-electrode devices with a symmetric Ag/1 SC/Ag architecture, with Ag electrodes aligned parallel to the polar c-axis (Figure 2a). Since high resistivity could effectively reduce current noise and dark current,

which was of great significance for exceptional-efficiency, X-ray detection. Therefore, by fit-ting the I-V curve, a superfor resistivity value of $1.45 \times 10^{11} \Omega$ cm for single crystal 1 was obtained (Figure 2b). Figure S7 depicts the wavelength dependence of the spectral photoresponse. Under the same light power density (2 mW cm⁻²), an excellent photoresponse (Ilight) was obtained at 520 nm. Thus, this wavelength was chosen as the characteristic wavelength for further evaluation of the photodetection performance. Figure 2c illustrates the current-voltage (I-V) characteristics measured along the c-axis under dark conditions and 520 nm illumination. The symmetry and linear behavior indicate good ohmic contact between the single crystal and the silver electrodes with a very small contact resistance. In particular, our SC devices exhibited a rather low dark current of approximately 20.9 pA. Such a low value of Idark was highly beneficial for a high detectivity, and the measured corresponding photocurrent (I_{ph}) increased rapidly with the increase in light intensity. Under an illumination of 233 mW cm⁻², the open-circuit photovoltage (V_{oc}) was approximately 0.15 V, and the I_{ph} was as high as 0.12 μ A. The on/off ratio was calculated to be 5.74×10³ (Figure 2c). Furthermore, the responsivity (R) and detectivity (D^*) , which are important indicators for evaluating the sensitivity of a detector, were calculated to be 35.3 mA W⁻¹ and 1.47×10^{12} Jones (5.38 μ W cm⁻²) respectively (Figure 2d). These results validate its significant potential in self-driven and highly efficient photodetection applications.

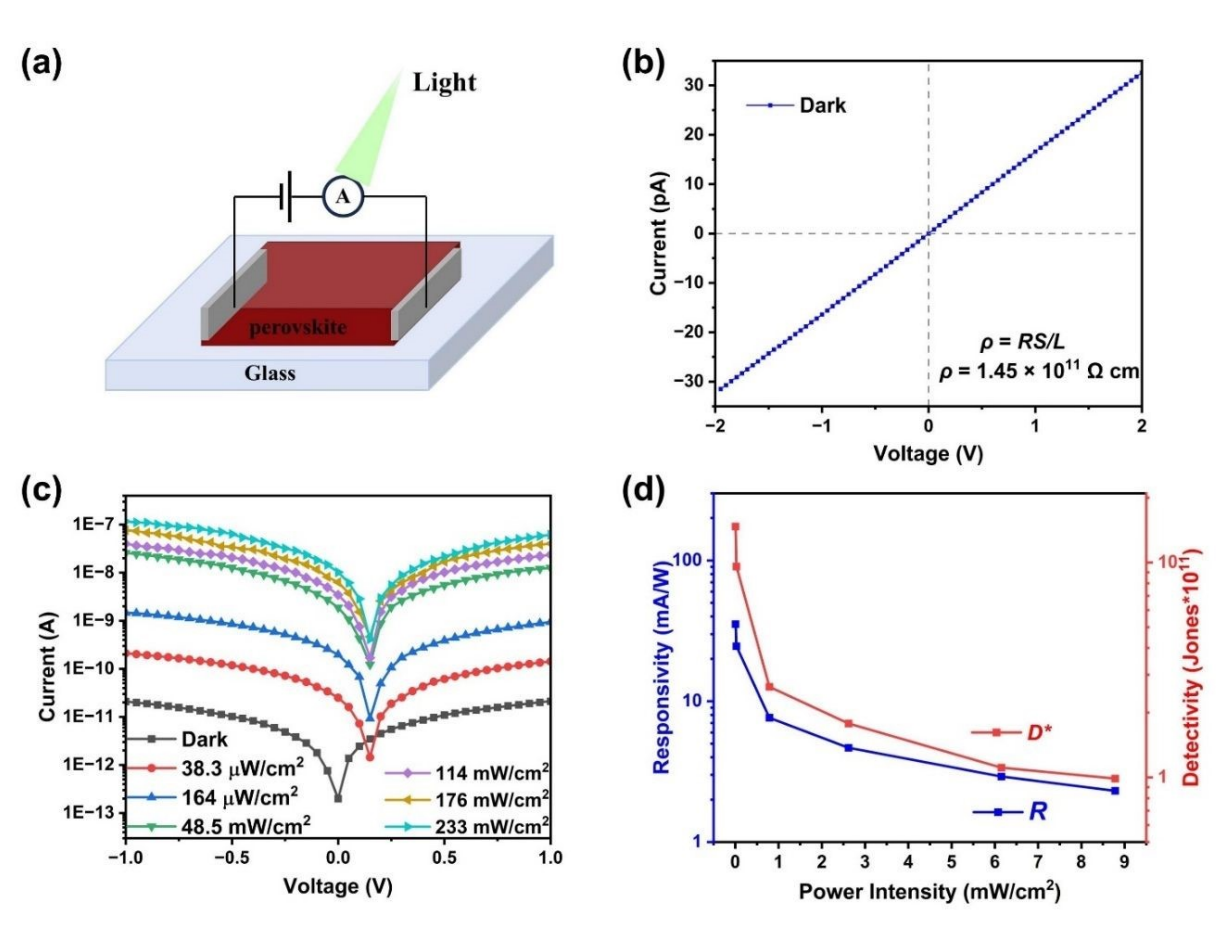


Fig. 2 (a) Device schematic of the lateral two-electrode detection devices constructed with SC of 1. (b) The resistivity of 1. (c) The I-V curves under 520 nm irradiation. (d) Responsivity and detectivity under 520 nm with different illumination power.

Journal Name ARTICLE

Considering the excellent self-driven photoelectric detection performance in the visible light range, combined with the advantages such as high Z element content, and high resistivity, 1 exhibits very good prospects in superior efficiency X-ray detection. Consequently, we systematically compared the X-ray attenuation properties of 1 with conventional detector materials across a broad energy spectrum (10 keV to 10 MeV) through photon cross-section database analysis (Figure 3a). 1 exhibited significantly enhanced X-ray absorption compared to Si, reaching performance levels comparable to CdTe. Attenuation analysis revealed that a 1 mm thickness of 1 could efficiently attenuate 97.4% of incident X-ray photons, demonstrating exceptional detection suitability (Figure 3b). In addition, charge collection capability is critical for achieving superior-performance detectors, which can be evaluated by μτ. We fitted the

current-voltage (*I-V*) curves of **1** and (*I-BA*)₂Pbl₄, under to X-FANY irradiation based on the modified Hecht equation. As shown in Figure 3c, the calculated value of μτ for **1** was greater than that of (*I-BA*)₂Pbl₄. This indicates that the two-dimensional multi-layer structure of **1** has great potential in achieving higher charge collection efficiency.³⁹ Besides, the polar structure endows **1** with remarkable spontaneous polarization characteristics. The polarization-induced built-in electric field enables **1** to automatically and directionally separate and transport photogenerated carriers, thus exhibiting the bulk photovoltaic effect.⁴⁰ Consequently, the self-driven X-ray response of the device under zero-bias conditions was performed. Consistent with predictions, **1** exhibited an obvious radiation-induced photovoltage of 0.15 V under X-ray exposure, establishing a built-in electric field for autonomous charge separation and enabling self-driven X-ray detection (Figure 3d).

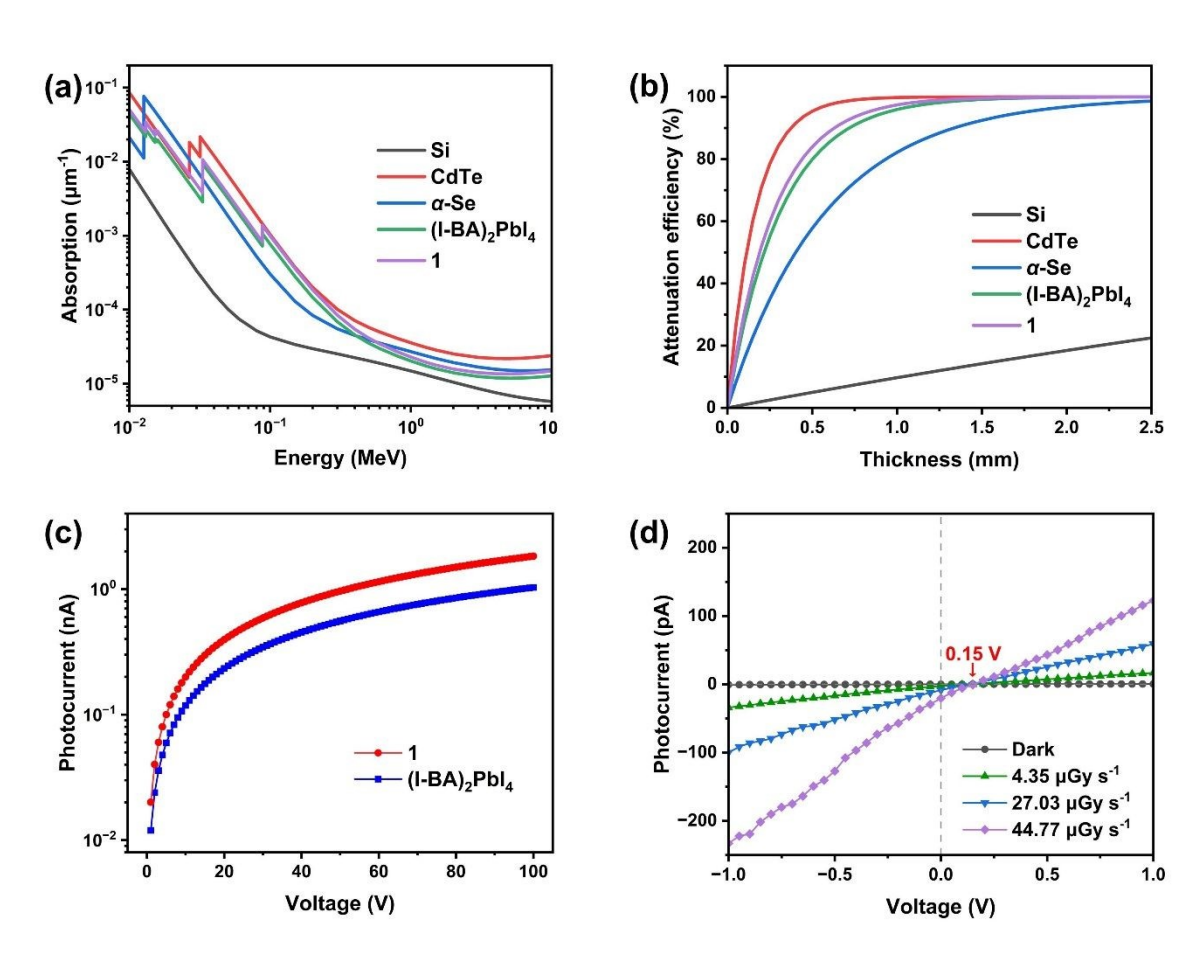


Fig. 3 (a) The X-ray absorption coefficient of Si, CdTe, α -Se, (I-BA)₂PbI₄ and **1**. (b) The attenuation efficiency of Si, CdTe, α -Se, (I-BA)₂PbI₄ and **1** at 50 keV photon energy. (c) The mobility-lifetime product of **1** and (I-BA)₂PbI₄. (d) *I-V* characteristics of **1** under X-ray illumination.

Figure 4a demonstrates a pronounced enhancement in photocurrent density from detector ${\bf 1}$ as the X-ray dose rate escalated from 4.35 to 44.77 μ Gy s⁻¹ under zero-bias conditions, confirming its superior radiation responsiveness. By fitting the current density corresponding to different dose rates at 0 V bias, the measured sensitivity was 221.7 μ C Gy⁻¹ cm⁻². This value exceeds that of some reported hybrid perovskites in self-driven mode, such as (*R*-PPA)(IEA)PbBr₄ (48.4 μ C Gy⁻¹ cm⁻²),⁴¹ (S-BPEA)₂FAPb₂I₇ (87.8 μ C Gy⁻¹ cm⁻²)⁴² and (IEA)₂FAPb₂I₇ (157.6 μ C Gy⁻¹ cm⁻²).⁴³ Moreover, as depicted in Figure 4b and c, owing to enhanced charge extraction with applied bias, at the same X-ray dose, the photocurrent density of detector **1** gradually increased with the enhancement of the external electric field. When the bias voltage grew from 10 V up to 50 V, the sensitivity rose substantially from 1558.4 μ C Gy⁻¹ cm⁻², highlighting its potential in X-ray detection research.⁴⁴

ARTICLE

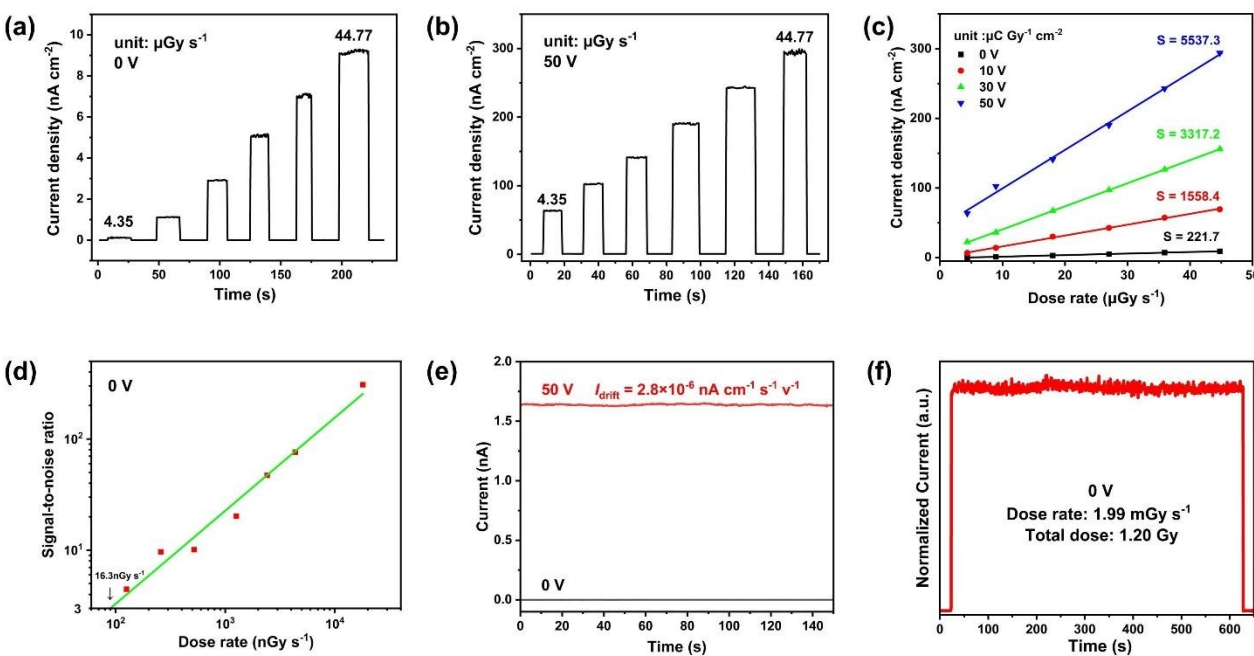


Fig. 4 (a,b) Current density-time curves for 1 detector under varying X-ray dose rates at 0 and 50 V bias, respectively. (c) The photocurrent densities at different bias voltages as a function of X-ray dose rates. (d) The SNR of 1 SC detector under different X-ray dose rates at zero bias indicates an ultra-low LoD of 16.3 nGy s⁻¹. (e) The I_{drift} at 0 V and 50 V. (f) The photocurrent response of 1 SC device during continuous X-ray irradiation.

Time (s)

The detection limit is another important parameter for evaluating the performance of X-ray detectors. 45, 46 The detection limit is formally defined by the International Union of Pure and Applied Chemistry (IUPAC) as the X-ray dose rate required to yield a signal exceeding noise levels by a factor of three. We recorded the current density-time (J-t) curve of the device under X-ray irradiation at a lower dose rate (Figure S8, Supporting Information) and calculated the corresponding signal-to-noise ratio. Therefore, the detection limit of 1 at 0 V bias was calculated in Figure 4d. Significantly, even at the ultra-low dose rate of 125.8 nGy s⁻¹, the system maintained an exceptional SNR of 4.46. Quantitative analysis established a LoD of 16.3 nGy s⁻¹, outperforming standard medical X-ray requirements (5.5 μ Gy s⁻¹)⁴⁷ by a factor of 337. This characteristic is extremely beneficial for practical medical imaging applications and in line with the pursuit of minimizing radiation hazards in the modern medical field. Figure 4e shows the dark current drift (Idrift) of detector 1. Even with a substantial external bias of 50 V applied, the device exhibited a moderate I_{drift} (2.8×10⁻⁶ nA cm⁻¹ s⁻¹ V⁻¹), particularly given its minimal and extremely stable dark current, which further highlights the merits of the self-driven detection. The detector based on ${\bf 1}$ was also exposed to continuous X-ray radiation to evaluate its radiation stability. 48, 49 The photocurrent and dark current remained stable under X-ray irradiation with a total accumulated dose of up to 1.20 Gy (Figure 4f), highlighting its excellent irradiation stability.

Conclusions

In summary, we reported a multilayer metal halide perovskite with halogenated amines as large spacer cations. The combination of the multilayer structure of the lead iodide inorganic framework and the halogenated amine cations endowed 1 with a polar structure, excellent electrical properties, and a narrow bandgap of 1.72 eV. Specifically, even without bias voltage, an outstanding responsivity of 35.3 mA W-1, and a detectivity of 1.47×10¹² Jones were achieved under illumination at 520 nm. In addition, 1 demonstrated outstanding self-driven X-ray detection capabilities with a high sensitivity of 221.7 μC Gy⁻¹ cm⁻² and a low detection limit of 16.3 nGy s-1. All these merits indicate that 1 is a prominent material for high-performance self-driven X-ray detection and provide insights into the design of 2D perovskites for self-driven photodetection.

Author contributions

Haotian Wen: design of the study, data collection and analysis, and writing - original draft. Minmin Wang: data analysis. Xin Dong: data analysis and writing - review & editing. Zhijin Xu: data analysis. Yaru Geng: data analysis. Jie Qin: data analysis. Junhua Luo: resources, project administration, and funding acquisition. Min Zhang: resources and project administration. Lina Li: resources, project administration, writing - review & editing, and supervision.

This article is licensed under a Creative Commons Attribution-NonCommercial 3.0 Unported Licence

Open Access Article. Published on 12 November 2025. Downloaded on 11/23/2025 5:16:22 PM

11.

ARTICLE

Conflicts of interest

There are no conflicts to declare.

Data availability

Supporting Information is available from the author.

Acknowledgements

This work was financially supported by NSFC (22322506 and 22175177), the NSF of Fujian Province (2023J06052), the Key Research Program of Frontier Sciences of the Chinese Academy of Sciences (ZDBS-LY-SLH024).

Notes and references

- R. Zhuang, X. Wang, W. Ma, Y. Wu, X. Chen, L. Tang, H. Zhu, J. Liu, L. Wu, W. Zhou, X. Liu and Y. Yang, Highly sensitive X-ray detector made of layered perovskite-like (NH₄)₃Bi₂l₉ single crystal with anisotropic response, *Nature Photonics*, 2019, 13, 602-608.
- X. Geng, Y.-A. Chen, Y.-Y. Li, J. Ren, G.-H. Dun, K. Qin, Z. Lin, J. Peng, H. Tian, Y. Yang, D. Xie and T.-L. Ren, Lead-Free Halide Perovskites for Direct X-Ray Detectors, *Advanced Science*, 2023, 10, 2300256.
- 3. H. Wu, Y. Ge, G. Niu and J. Tang, Metal Halide Perovskites for X-Ray Detection and Imaging, *Matter*, 2021, **4**, 144-163.
- Y. He, J. Song, M. Li, K. Sakhatskyi, W. Li, X. Feng, B. Yang, M. Kovalenko and H. Wei, Perovskite computed tomography imager and three-dimensional reconstruction, *Nature Photonics*, 2024, 18, 1052-1058.
- Y. C. Kim, K. H. Kim, D.-Y. Son, D.-N. Jeong, J.-Y. Seo, Y. S. Choi, I. T. Han, S. Y. Lee and N.-G. Park, Printable organometallic perovskite enables large-area, low-dose Xray imaging, *Nature*, 2017, 550, 87-91.
- J. Jiang, M. Xiong, K. Fan, C. Bao, D. Xin, Z. Pan, L. Fei, H. Huang, L. Zhou, K. Yao, X. Zheng, L. Shen and F. Gao, Synergistic strain engineering of perovskite single crystals for highly stable and sensitive X-ray detectors with low-bias imaging and monitoring, *Nature Photonics*, 2022, 16, 575-581.
- 7. W. Pan, H. Wu, J. Luo, Z. Deng, C. Ge, C. Chen, X. Jiang, W.-J. Yin, G. Niu, L. Zhu, L. Yin, Y. Zhou, Q. Xie, X. Ke, M. Sui and J. Tang, Cs₂AgBiBr₆ single-crystal X-ray detectors with a low detection limit, *Nature Photonics*, 2017, **11**, 726-732.
- 8. W. Guo, X. Liu, S. Han, Y. Liu, Z. Xu, M. Hong, J. Luo and Z. Sun, Room-Temperature Ferroelectric Material Composed of a Two-Dimensional Metal Halide Double Perovskite for X-ray Detection, *Angewandte Chemie International Edition*, 2020, **59**, 13879-13884.
- Y. Shen, Y. Liu, H. Ye, Y. Zheng, Q. Wei, Y. Xia, Y. Chen, K. Zhao, W. Huang and S. Liu, Centimeter-Sized Single Crystal of Two-Dimensional Halide Perovskites Incorporating Straight-Chain Symmetric Diammonium Ion for X-Ray Detection, Angewandte Chemie International Edition, 2020, 59, 14896-14902.
- C. Ma, S. Wang, L. Gao, Z. Xu, X. Song, T. Yang, H. Li, X. Liu,
 S. Liu and K. Zhao, Halide-Initiated Structural Regulation in Amidino-Based Low-Dimensional Perovskite/Perovskitoid

and Their Application for Crystal X-Ray Detectors. Advanced Optical Materials, 2023, 11,12202449050101912E H. Wei, Y. Fang, P. Mulligan, W. Chuirazzi, H.-H. Fang, C. Wang, B. R. Ecker, Y. Gao, M. A. Loi, L. Cao and J. Huang, Sensitive X-ray detectors made of methylammonium lead tribromide perovskite single crystals, Nature Photonics, 2016, 10, 333-339.

Journal Name

- 12. P.-J. Huang, K. Taniguchi and H. Miyasaka, Bulk Photovoltaic Effect in a Pair of Chiral–Polar Layered Perovskite-Type Lead Iodides Altered by Chirality of Organic Cations, *Journal of the American Chemical Society*, 2019, **141**, 14520-14523.
- C.-K. Yang, W.-N. Chen, Y.-T. Ding, J. Wang, Y. Rao, W.-Q. Liao, Y.-Y. Tang, P.-F. Li, Z.-X. Wang and R.-G. Xiong, The First 2D Homochiral Lead Iodide Perovskite Ferroelectrics: [R- and S-1-(4-Chlorophenyl)ethylammonium]₂Pbl₄, Advanced Materials, 2019, 31, 1808088.
- S. Shrestha, R. Fischer, G. J. Matt, P. Feldner, T. Michel, A. Osvet, I. Levchuk, B. Merle, S. Golkar, H. Chen, S. F. Tedde, O. Schmidt, R. Hock, M. Rührig, M. Göken, W. Heiss, G. Anton and C. J. Brabec, High-performance direct conversion X-ray detectors based on sintered hybrid lead triiodide perovskite wafers, *Nature Photonics*, 2017, 11, 436-440.
- I.-H. Park, K. C. Kwon, Z. Zhu, X. Wu, R. Li, Q.-H. Xu and K. P. Loh, Self-Powered Photodetector Using Two-Dimensional Ferroelectric Dion–Jacobson Hybrid Perovskites, *Journal of the American Chemical Society*, 2020, 142, 18592-18598.
- Y.-Y. Tang, W.-Y. Zhang, P.-F. Li, H.-Y. Ye, Y.-M. You and R.-G. Xiong, Ultrafast Polarization Switching in a Biaxial Molecular Ferroelectric Thin Film: [Hdabco]ClO₄, Journal of the American Chemical Society, 2016, 138, 15784-15789.
- 17. X. Dong, J. Liang, Z. Xu, H. Wu, L. Wang, S. You, J. Luo and L. Li, Exploring centimeter-sized crystals of bismuth-iodide perovskite toward highly sensitive X-ray detection, *Chinese Chemical Letters*, 2024, **35**, 108708.
- S. You, Z.-K. Zhu, S. Dai, J. Wu, Q. Guan, T. Zhu, P. Yu, C. Chen, Q. Chen and J. Luo, Inch-Size Single Crystals of Lead-Free Chiral Perovskites with Bulk Photovoltaic Effect for Stable Self-Driven X-Ray Detection, Advanced Functional Materials, 2023, 33, 2303523.
- C.-C. Fan, X.-B. Han, B.-D. Liang, C. Shi, L.-P. Miao, C.-Y. Chai, C.-D. Liu, Q. Ye and W. Zhang, Chiral Rashba Ferroelectrics for Circularly Polarized Light Detection, Advanced Materials, 2022, 34, 2204119.
- J. Yan, F. Gao, Y. Tian, Y. Li, W. Gong, S. Wang, H. Zhu and L. Li, Controllable Perovskite Single Crystal Heterojunction for Stable Self-Powered Photo-Imaging and X-Ray Detection, Advanced Optical Materials, 2022, 10, 2200449.
- 21. X. Zhang, T. Zhu, C. Ji, Y. Yao and J. Luo, In Situ Epitaxial Growth of Centimeter-Sized Lead-Free (BA)₂CsAgBiBr₇/Cs₂AgBiBr₆ Heterocrystals for Self-Driven X-ray Detection, *Journal of the American Chemical Society*, 2021, **143**, 20802-20810.
- 22. X. Zhang, L. Li, C. Ji, X. Liu, Q. Li, K. Zhang, Y. Peng, M. Hong and J. Luo, Rational design of high-quality 2D/3D perovskite heterostructure crystals for recordperformance polarization-sensitive photodetection, National Science Review, 2021, 8, nwab044.
- K. Tao, C. Xiong, J. Lin, D. Ma, S. Lin, B. Wang and H. Li, Self-Powered Photodetector Based on Perovskite/NiO_x
 Heterostructure for Sensitive Visible Light and X-Ray

This article is licensed under a Creative Commons Attribution-NonCommercial 3.0 Unported Licence.

Open Access Article. Published on 12 November 2025. Downloaded on 11/23/2025 5:16:22 PM

Journal Name ARTICLE

37.

38.

- Detection, Advanced Electronic Materials, 2023, 9, 2201222.
- 24. X. Wang, Y. Li, Y. Xu, Y. Pan, C. Zhu, D. Zhu, Y. Wu, G. Li, Q. Zhang, Q. Li, X. Zhang, J. Wu, J. Chen and W. Lei, Solution-Processed Halide Perovskite Single Crystals with Intrinsic Compositional Gradients for X-ray Detection, *Chemistry of Materials*, 2020, 32, 4973-4983.
- 25. T. Zhu, W. Weng, C. Ji, X. Zhang, H. Ye, Y. Yao, X. Li, J. Li, W. Lin and J. Luo, Chain-to-Layer Dimensionality Engineering of Chiral Hybrid Perovskites to Realize Passive Highly Circular-Polarization-Sensitive Photodetection, *Journal of the American Chemical Society*, 2022, 144, 18062-18068.
- J. Wu, S. You, P. Yu, Q. Guan, Z.-K. Zhu, Z. Li, C. Qu, H. Zhong,
 L. Li and J. Luo, Chirality Inducing Polar Photovoltage in a
 2D Lead-Free Double Perovskite toward Self-Powered X-ray Detection, ACS Energy Letters, 2023, 8, 2809-2816.
- 27. T. Schmitt, S. Bourelle, N. Tye, G. Soavi, A. D. Bond, S. Feldmann, B. Traore, C. Katan, J. Even, S. E. Dutton and F. Deschler, Control of Crystal Symmetry Breaking with Halogen-Substituted Benzylammonium in Layered Hybrid Metal-Halide Perovskites, *Journal of the American Chemical Society*, 2020, 142, 5060-5067.
- A. Morteza Najarian, F. Dinic, H. Chen, R. Sabatini, C. Zheng,
 A. Lough, T. Maris, M. I. Saidaminov, F. P. García de Arquer,
 O. Voznyy, S. Hoogland and E. H. Sargent, Homomeric chains of intermolecular bonds scaffold octahedral germanium perovskites, *Nature*, 2023, 620, 328-335.
- 29. M. L. Ball, J. V. Milić and Y.-L. Loo, The Emerging Role of Halogen Bonding in Hybrid Perovskite Photovoltaics, *Chemistry of Materials*, 2022, **34**, 2495-2502.
- 30. T. Sheikh, S. Maqbool, P. Mandal and A. Nag, Introducing Intermolecular Cation-π Interactions for Water-Stable Low Dimensional Hybrid Lead Halide Perovskites, *Angewandte Chemie International Edition*, 2021, **60**, 18265-18271.
- 31. Y. Liu, S. Han, J. Wang, Y. Ma, W. Guo, X.-Y. Huang, J.-H. Luo, M. Hong and Z. Sun, Spacer Cation Alloying of a Homoconformational Carboxylate trans Isomer to Boost in-Plane Ferroelectricity in a 2D Hybrid Perovskite, *Journal of the American Chemical Society*, 2021, **143**, 2130-2137.
- 32. T. Chen, W. Yang, C. Shi, Z. Xu, X. Dong, J. Liang, J. Luo and L. Li, Mn(II)-Doped Perovskites with Carboxylic Acid Dimers Exhibiting Scintillation, *Inorganic Chemistry*, 2025, **64**, 5652-5660.
- 33. H. Li, W. Jiang, J. Wu, J. Ren, Y. Zhao, D. Liu, Z. Hu and Y. Zhao, Ultralow Ion Migration and X-Ray Response from Strong Dipole Moments in (Br-EA)₂PbBr₄ Perovskite Single Crystals, *Small*, 2025, **21**, 2406722.
- 34. J. Xue, Y. Huang, Y. Liu, Z. Chen, H. H. Y. Sung, I. D. Williams, Z. Zhu, L. Mao, X. Chen and H. Lu, Rashba Band Splitting and Bulk Photovoltaic Effect Induced by Halogen Bonds in Hybrid Layered Perovskites, *Angewandte Chemie International Edition*, 2023, 62, e202304486.
- D. Li, W. Wu, S. Han, X. Liu, Y. Peng, X. Li, L. Li, M. Hong and J. Luo, A reduced-dimensional polar hybrid perovskite for self-powered broad-spectrum photodetection, *Chemical Science*, 2021, 12, 3050-3054.
- C. C. Stoumpos, D. H. Cao, D. J. Clark, J. Young, J. M. Rondinelli, J. I. Jang, J. T. Hupp and M. G. Kanatzidis, Ruddlesden–Popper Hybrid Lead Iodide Perovskite 2D Homologous Semiconductors, *Chemistry of Materials*, 2016, 28, 2852-2867.

- J. M. Hoffman, C. D. Malliakas, S. Sidhik, Hadar Alike McClain, A. D. Mohite and M. G. Kanatzidis 100g periodic ripple in a 2D hybrid halide perovskite structure using branched organic spacers, *Chemical Science*, 2020, **11**, 12139-12148.
- J. M. Hoffman, X. Che, S. Sidhik, X. Li, I. Hadar, J.-C. Blancon, H. Yamaguchi, M. Kepenekian, C. Katan, J. Even, C. C. Stoumpos, A. D. Mohite and M. G. Kanatzidis, From 2D to 1D Electronic Dimensionality in Halide Perovskites with Stepped and Flat Layers Using Propylammonium as a Spacer, *Journal of the American Chemical Society*, 2019, 141, 10661-10676.
- X. Li, J. Hoffman, W. Ke, M. Chen, H. Tsai, W. Nie, A. D. Mohite, M. Kepenekian, C. Katan, J. Even, M. R. Wasielewski, C. C. Stoumpos and M. G. Kanatzidis, Two-Dimensional Halide Perovskites Incorporating Straight Chain Symmetric Diammonium Ions, (NH₃C_mH_{2m}NH₃)(CH₃NH₃)_{n-1}Pb_nI_{3n+1} (m = 4–9; n = 1–4), Journal of the American Chemical Society, 2018, 140, 12226-12238.
- L. Guo, X. Liu, L. Gao, X. Wang, L. Zhao, W. Zhang, S. Wang,
 C. Pan and Z. Yang, Ferro-Pyro-Phototronic Effect in Monocrystalline 2D Ferroelectric Perovskite for High-Sensitive, Self-Powered, and Stable Ultraviolet Photodetector, ACS Nano, 2022, 16, 1280-1290.
- Z.-K. Zhu, J. Wu, P. Yu, Y. Zeng, R. Li, Q. Guan, H. Dai, G. Chen, H. Yang, X. Liu, L. Li, C. Ji and J. Luo, Polar Alternating Cations Intercalated Hybrid Perovskite with Iodine-Substituted Spacers Toward Efficient Passive X-Ray Detection, Advanced Functional Materials, 2024, 34, 2409857.
- Q. Guan, H. Ye, S. You, Z.-K. Zhu, H. Li, X. Liu and J. Luo, Radiation Photovoltaics in a 2D Multilayered Chiral-Polar Halide Perovskite toward Efficient Self-Driven X-Ray Detection, Small, 2024, 20, 2307908.
- D. Fu, Y. Zhang, Z. Chen, L. Pan, Y. He and J. Luo, Bulk Photovoltaic Effect Induced by Non-Covalent Interactions in Bilayered Hybrid Perovskite for Efficient Passive X-Ray Detection, Small, 2024, 20, 2403198.
- W. Pan, W. Li, J. Zong, H. Hu, K. Guo, C. Li, W. Qu and H. Wei, A Low-Dimensional Donor-Acceptor Perovskite for High-Performance X-Ray Detection, Advanced Functional Materials, 2025, 35, 2414553.
- 45. Y. Liu, Z. Xu, Z. Yang, Y. Zhang, J. Cui, Y. He, H. Ye, K. Zhao, H. Sun, R. Lu, M. Liu, M. G. Kanatzidis and S. Liu, Inch-Size OD-Structured Lead-Free Perovskite Single Crystals for Highly Sensitive Stable X-Ray Imaging, *Matter*, 2020, **3**, 180-196.
- 46. A. Glushkova, P. Andričević, R. Smajda, B. Náfrádi, M. Kollár, V. Djokić, A. Arakcheeva, L. Forró, R. Pugin and E. Horváth, Ultrasensitive 3D Aerosol-Jet-Printed Perovskite X-ray Photodetector, ACS Nano, 2021, 15, 4077-4084.
- 47. Y. Zhang, Y. Liu, Z. Xu, H. Ye, Z. Yang, J. You, M. Liu, Y. He, M. G. Kanatzidis and S. Liu, Nucleation-controlled growth of superior lead-free perovskite Cs₃Bi₂I₉ single-crystals for high-performance X-ray detection, *Nature Communications*, 2020, **11**, 2304.
- X. Feng, L. Zhang, X. Feng, J. You, J. Pi, H. Zeng, D. Chu, C. Xue, K. Zhao, S. Jia, P. Tong, Z. Jin, Y. Liu, A. K. Y. Jen and S. F. Liu, Ion Migration Suppression via Doping Multivalent Cations in Perovskite for High Thermal Stability X-ray Detectors, ACS Energy Letters, 2025, 10, 685-695.

This article is licensed under a Creative Commons Attribution-NonCommercial 3.0 Unported Licence.

Open Access Article. Published on 12 November 2025. Downloaded on 11/23/2025 5:16:22 PM.

ARTICLE

Journal Name

49. X. Zheng, W. Zhao, P. Wang, H. Tan, M. I. Saidaminov, S. Tie, L. Chen, Y. Peng, J. Long and W.-H. Zhang, Ultrasensitive and stable X-ray detection using zerodimensional lead-free perovskites, Journal of Energy Chemistry, 2020, 49, 299-306.

View Article Online DOI: 10.1039/D5QI01912E Journal Name ARTICLE

This article is licensed under a Creative Commons Attribution-NonCommercial 3.0 Unported Licence.

Open Access Article. Published on 12 November 2025. Downloaded on 11/23/2025 5:16:22 PM.

View Article Online DOI: 10.1039/D5QI01912E

View Article Online DOI: 10.1039/D5QI01912E

Data Availability Statement

The data that support the findings of this study are available from the corresponding author upon reasonable request.